

Supplemental Information

BRCA2 coordinates the activities of cell cycle kinases to promote genome stability

Keiko Yata, Jean-Yves Bleuyard, Ryuichiro Nakato, Christine Ralf, Yuki Katou, Rebekka A Schwab, Wojciech Niedzwiedz, Katsuhiko Shirahige and Fumiko Esashi

Inventory of Supplemental Information

Supplemental Discussion

Supplemental Experimental Procedures

Figure S1, related to Figure 1

Figure S2, related to Figure 2

Figure S3, related to Figure 3

Figure S4, related to Figure 4

Figure S5, related to Figure 5

Figure S6, related to Figure 6

Table S1, related to Experimental Procedures

Supplemental References

Supplemental Discussion

This study and our previous work (Yata et al., 2012) demonstrate the importance of Rad51 S14 phosphorylation in the maintenance of genome stability during DNA damage and replicative stress responses. The kinase(s) responsible for this phosphorylation are of immense interest. We have previously shown that Plk1 directly phosphorylates Rad51 at S14 *in vitro* (Yata et al., 2012), and our data so far indicate that S14 phosphorylation of Rad51 is primarily mediated by Plk1 *in vivo*. Specifically: 1) reduced pS14 was detected following small molecule Plk1 inhibitor treatment (Yata et al., 2012); 2) pS14 increased in abundance as the activity of Plk1 increased during cell cycle progression (Yata et al., 2012); 3) unlike cells arrested in mitosis due to prolonged treatment with a CDK1 inhibitor or nocodazole (Yata et al., 2012), cells arrested in mitosis by siRNA mediated down-regulation of Plk1 exhibited no increase in the level of pS14 (Yata and Esashi, unpublished data); 4) in a cell line expressing a mutant Plk1 that can be conditionally inactivated by the ATP analogue NM1-PP1 (Burkard et al., 2007), the pS14 level was unchanged upon NM1-PP1 treatment, despite accumulation of these cells in mitosis (Ronson and Esashi, unpublished data); 5) siRNA-mediated down-regulation of other Polo-like kinase family members such as Plk2 and Plk3, which are active in interphase (Barr et al., 2004), has minimal effects on the cell cycle profile and did not alter Rad51 S14 phosphorylation (Yata and Esashi, unpublished data); and 6) selective BRCA2 interaction with Plk1, but not with Plk2 nor Plk3, was detectable under the conditions we employed (Fig. S2I). We believe our studies provide strong evidence in support of the view that BRCA2 facilitates Plk1-dependent Rad51 phosphorylation by acting as a platform, and that this contributes to genome stability control, although the potential involvement of other kinase(s) in Rad51 phosphorylation under other circumstances should be addressed in future studies.

Supplemental Experimental Procedures

***In vitro* kinase reactions and far-western blotting**

For *in vitro* kinase assays, recombinant proteins (5 µg in 20 µl total volume) were phosphorylated with ~40 ng of recombinant CDK2/cyclin A (kind gift from Prof. Jane Endicott and Dr. Aude Echaliier) in Kinase Buffer (5 mM HEPES pH 7.6, 25 mM NaCl, 25 mM β-glycerophosphate, 5 mM MgCl₂, 5 mM MnCl₂, 1 mM DTT) supplemented with 50 µM ATP for 10 min at 30°C. Following SDS-PAGE, proteins were transferred to a Protran nitrocellulose membrane (BA85, Whatman) and incubated with purified recombinant Plk1-PBD (~1.5 µg per reaction) and anti-Plk1 antibody for 16 hours at 4°C. Quantification of autoradiographs and immunoblots were carried out using ImageJ software (Rasband, W.S., ImageJ, U. S. National Institutes of Health).

Extract preparation, cellular fractionation, and immunoprecipitation

Preparations of whole cell extract, cellular fractionation and immunoprecipitation were carried out as previously described (Bleuyard et al., 2012; Yata et al., 2012). Where indicated, the membrane was treated with Re-Blot Plus Mild Solution (Merck Millipore) before incubating with another antibody; for Rad51 phosphorylation analyses, anti-pT13/pS14, anti-pS14, and anti-Rad51 antibodies were applied in this order. For BRCA2 analysis, anti-pT77 was first applied, followed by anti-BRCA2 antibody.

DNA fibre analysis

U2OS cells exogenously expressing Rad51 variants were treated with siRNA to down-regulate endogenous Rad51. Cells were then pulse-labeled with 25 µM 5'iodo-2'deoxyuridine (IdU) (Sigma-Aldrich) for 20 min. After IdU was washed out, cells were treated with 4 mM HU for 4 hours, followed by 1 hour pulse-labeling with 250 µM 5'chloro-2'deoxyuridine (CldU) (Sigma-Aldrich). Cells were harvested, lysed and spread on microscope slides as previously described (Jackson

and Pombo, 1998; Schwab et al., 2010). Fibre tracts were immuno-labeled with mouse BD 347580 antibody (for IdU) and rat ab6326 antibody (for CldU). The images were taken with an Olympus BX60 microscope (Cambridge Research) and using CRi Nuance Multispectral Imaging System version 2.10.0 software. A minimum of 150 DNA tracts were analysed from each experiment using ImageJ software and at least three independent experiments were performed. *p*-values were determined from the Student's unpaired two-tailed t-test using Prism software (GraphPad Software).

Plasmids

cDNA of Plk1 (HsCD00003326, Life Technologies) was used as template for PCR cloning of Plk1 and Plk1-PBD with a PreScission protease proteolytic site at the 5' end in pDONR221, and transferred to pDEST15 and pDEST27 (Life Technologies) for GST-fusion expression in bacteria and mammalian cells, respectively. BRCA2 fragments were cloned into pENTR1A at *Sall/NotI* sites, and transferred to pDEST17 and pDEST53 (Life Technologies) for bacterial expression as 6xHis fusions and mammalian expression as GFP fusions respectively. For 3xFLAG-fusion expression in mammalian cells, BRCA2 NTD in pENTR1A was transferred to pDESTa/FRT/N3xFLAG, a modified pcDNA5/FRT (Life Technologies) with an N3xFLAG cassette at *HindIII/XhoI* sites and a Gateway conversion site at *EcoRV*. Synthetic oligonucleotides for shRNA BRCA2 and Rad51 were annealed and cloned into pSUPERIOR.puro vector (Oligoengine) at *BglII/HindIII* sites.

Generation of full length BRCA2 with point mutations

To generate BRCA2 constructs, a *KpnI*-EGFP-*KpnI*-*NotI*-*XhoI* cassette was PCR cloned into the pFlp-In T-REx 1xFLAG vector, a modified pcDNA5/FRT/TO with a cassette comprising 1xFLAG and a Gateway conversion site at *PmeI*. Full length BRCA2 was then cloned at *NotI/XhoI* sites. For

full length BRCA2 variant with BRC mutations, point mutations were first introduced into pENTR1A-B2-3 or pENTR1A-B2-4, which respectively carry the corresponding B2-3 or B2-4 BRCA2 cDNA fragments of previously described pGEX4 constructs (Esashi et al., 2005) at *Sall/NotI* sites. Secondly, 1.2 kb of B2-3 cDNA with mutations was PCR amplified using primers 1 and 2, and cloned into N-terminal *Sall/NdeI* sites of B2-4 (product 1). Thirdly, ~3 kb of N-terminal BRCA2 cDNA fragment from wild-type full length BRCA2 was isolated using *KpnI* and *Eam1105I*, and introduced into N-terminal *KpnI/Eam1105I* sites in product 1 (product 2). Finally, ~5 kb N-terminal BRCA2 fragment from product 2 was cloned into *NotI/EcoRV* sites in full length BRCA2. For the full-length BRCA2 variant with T77A or A75P, three native *BamHI* sites within BRCA2 cDNA were modified and/or used. B2-1 cDNA with mutations was first PCR amplified using primers 3 and 4 to generate a fragment of 560 bp. This fragment was then cloned into *NotI/BamHI* sites of full length BRCA2, but with internal deletion arising from second and third native *BamHI* sites within the *BRCA2* gene. The internal 7.2 kb of the BRCA2 fragment arising from these two native *BamHI* sites was then re-introduced to generate full length BRCA2. Full length BRCA2 with S3291E mutation was generated by replacing C-terminal BRCA2 with a PCR amplified B2-9 cDNA with mutation using primers 5 and 6 at *SphI/XhoI* sites. All mutations were confirmed by sequencing.

Antibodies

Antibodies and related products were obtained from the following sources. Anti-BRCA2 (OP95, Calbiochem; ab9143, Abcam), anti-BrdU (347580, Beckton Dickinson; ab6326, Abcam; RPN 202, GE Healthcare), anti-Cyclin E (HE12, Cell Signaling), anti-FLAG-HRP (M2, Sigma-Aldrich), anti-GST (B-14, Santa Cruz), anti-GAPDH (G8545, Sigma-Aldrich), anti-GFP (G1544, Sigma-Aldrich), anti-H2A (2578, Cell Signaling), anti-H2A.X (2595, Cell Signaling; 07-627, Merck Millipore), anti- γ H2A.X (JBW301, Merck Millipore; 07-164, Merck Millipore), anti-Histone H3 (A300-823A, Bethyl Laboratories), anti-pS10 Histone H3 (06-570, Millipore), anti-HA tag (12CA5, Sigma-Aldrich) anti-

Lamin A (L1293, Sigma-Aldrich), anti-Nbs1 (N3037, Sigma-Aldrich), anti-PALB2 (A301-246A, Bethyl Laboratories), anti-PCNA (P8825, Sigma-Aldrich), anti-Plk1 (A300-251A, Bethyl Laboratories; 36-298, Sigma-Aldrich), anti-Rad51 (ab213, Abcam), anti-Tubulin (Tat1, Cancer Research UK), anti-mouse AlexaFluor 555-conjugated goat IgG, anti-rat AlexaFluor 488-conjugated goat IgG (Life Technologies), Rabbit IgG (02-6102, Life Technologies) and Protein A/G-HRP (32490, Thermo Scientific). Anti-Cyclin A (AT10.3) and anti-Cyclin B (V152) were kind gift from Dr. Tim Hunt. Anti-pS14 Rad51 and anti-pT13/pS14 Rad51 (Yata et al., 2012), anti-pS3291 (Esashi et al., 2005) were previously described. Anti-Rad51 rabbit polyclonal antibody (7946) was raised against full-length recombinant Rad51 protein (Biogenes).

Purification of recombinant proteins

Plk1 or Plk1-PBD in pDEST15 was transformed in BL21 Codon Plus -RIL *E. coli* (Agilent Technologies) and induced with 0.1 mM isopropyl β -D-thiogalactoside (IPTG) at 20°C for 12 hours. GST-fusion was purified using Glutathione Sepharose 4B (GE Healthcare) in MOPS buffered saline [200 mM NaCl, 40 mM MOPS, pH7.4, 0.5 mM TCEP, 0.01% NaN₃, supplemented with Protease Inhibitor Cocktail (Sigma-Aldrich, P2714) and 5 mM benzamidine hydrochloride], and GST-tag was cleaved with PreScission Protease treatment (GE Healthcare). His-fusion BRCA2 NTD plasmid was expressed as above except that protein expression was induced with incubation of 0.1 mM IPTG for 16 hours at 20°C. His-tagged recombinant protein was affinity purified with TALON Metal Affinity Resin (Clontech) in modified HEPES buffered saline [200 mM NaCl, 40 mM HEPES, pH7.0, 0.5 mM TCEP, 0.01% NaN₃, 20 mM imidazole, supplemented with cComplete EDTA-free protease inhibitor cocktail (Roche Applied Science) and 5 mM benzamidine hydrochloride].

Isolation of proteins on nascent DNA (iPOND)

5×10^7 HEK293T cells (per condition) were plated in two 15 cm plates the day before the experiment. On the following day, nascent DNA was labeled by addition of 10 μ M 5-ethynyl-2'-deoxyuridine (EdU, Life Technologies) to the medium for 15 min. For the thymidine chase condition, the EdU labeled cells were washed once and incubated for 30 min in pre-warmed thymidine chase medium (DMEM supplemented with 10% FBS and 10 μ M thymidine, Sigma-Aldrich). For the hydroxyurea (HU) chase condition, the EdU labeled cells were washed once and incubated for the indicated time in pre-warmed HU chase medium (DMEM supplemented with 10% FBS and 4 mM Hydroxyurea, Sigma-Aldrich). Next, cells were fixed for 5 min at room temperature by addition of 1/10 volume of 10% formaldehyde (Sigma-Aldrich)/PBS pH 7.2 (Life Technologies), and unreacted formaldehyde was quenched with Glycine (Sigma-Aldrich) at a final concentration of 125 mM for 5 min at room temperature. Cells were washed with PBS, permeabilized (0.25% Triton X-100 in PBS, 20 to 30 min at room temperature), and washed again with PBS. To perform the Click reaction, cells were incubated for 1.5 to 2 h in PBS supplemented with 10 mM (+)-sodium L-ascorbate (Sigma-Aldrich), 0.05 mM Biotin Azide (Life Technologies) and 2 mM copper (II) sulfate (Sigma-Aldrich), followed by addition of three volumes of PBS supplemented with 1% BSA and 0.5% Tween-20 and incubation for additional 10 min. After two washes in PBS, cells were extracted in CL lysis buffer (50 mM HEPES pH 7.6, 150 mM NaCl, 0.5% NP-40 alternative, 0.25% Triton X-100, 10% glycerol containing protease and phosphatase inhibitors), washed in iPOND wash buffer (10 mM Tris-HCl pH 8, 200 mM NaCl, 0.5 mM DTT containing protease and phosphatase inhibitors) and resuspended in RIPA buffer (50 mM Tris-HCl pH 8, 150 mM NaCl, 1% NP-40 alternative, 0.1% SDS, 0.5% Na-Deoxycholate containing protease and phosphatase inhibitors). Following sonication, the cell lysate was clarified by centrifugation at 16,100 g for 45 min at 4°C. Finally, Biotin-labeled DNA-protein complexes were pulled down using NeutrAvidin Plus UltraLink resin (Pierce). The resin was washed three times with iPOND wash buffer and

boiled 15 to 20 min at 99°C in NuPAGE LDS Sample Buffer (Life Technologies) containing 5% β -mercaptoethanol. Quantification of immunoblots was carried out using ImageJ software (Rasband, W.S., ImageJ, U.S. National Institutes of Health).

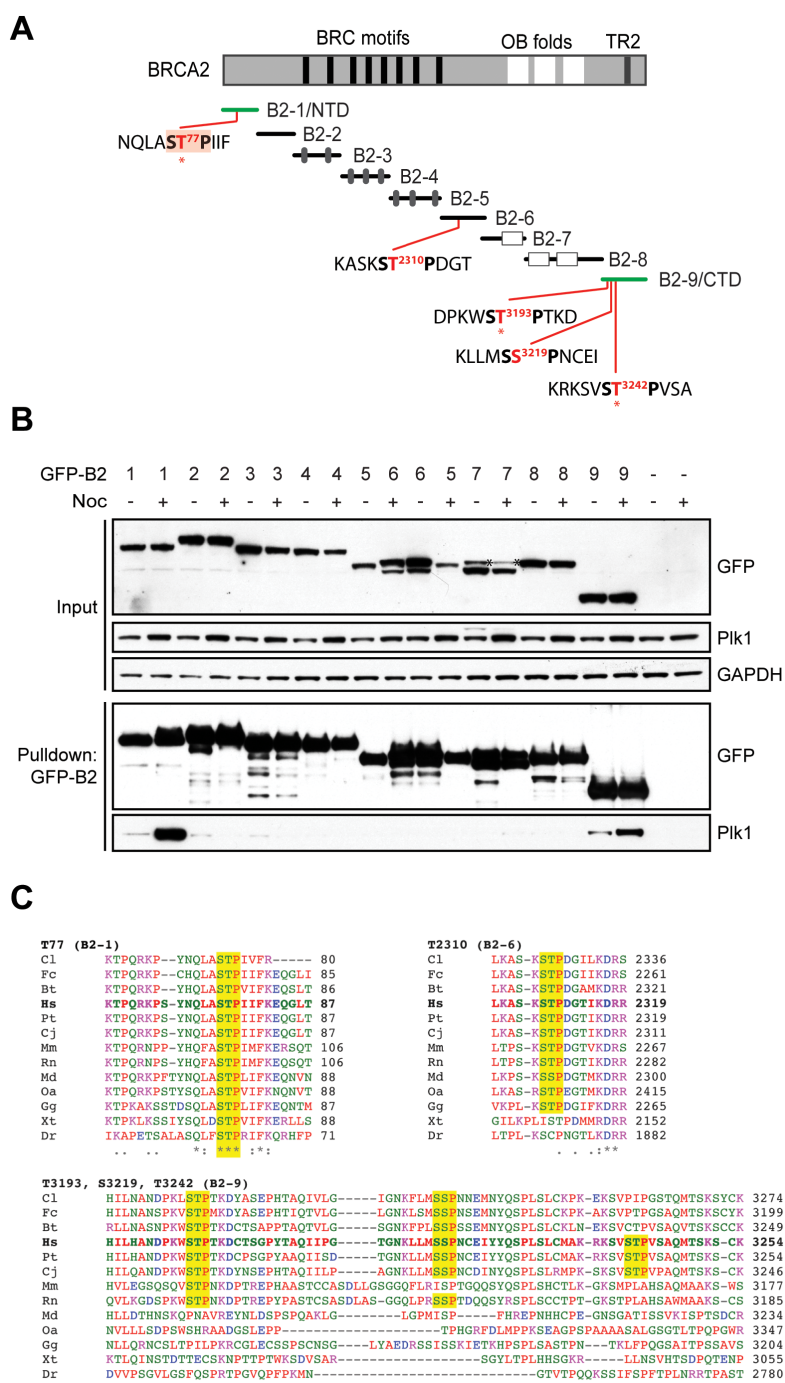


Figure S1, related to Figure 1. Potential *Pik1* binding motifs within *BRCA2*.

(A) Schematic diagram of the nine overlapping *BRCA2* fragments, designated B2-1 to B2-9, where fragments that are phosphorylated by recombinant CDK2/cyclin A experimentally are highlighted in green (Esashi et al., 2005). Minimal PBD-binding motifs with potential CDK phosphorylation sites (S-[pT/pS]-P) are indicated in bold on each fragment. Note that the motif within B2-6 contains lysine (K2308) at -2 position from the T2310 CDK target that may block PBD binding (Elia et al.,

2003). Red letters: potential CDK target sites, pink box: PBD binding site addressed in this study, asterisks: previously described phosphorylation sites (Cell Signaling Technology).

(B) GFP-fusions of BRCA2 fragments were exogenously expressed in HEK293T cells, and following GFP pull-down, their association to Plk1 was assessed by western blotting. Asterisks indicate non-specific bands.

(C) Multiple amino acid sequence alignment surrounding each PBD-binding motif within BRCA2 by ClustalW2 (<http://www.ebi.ac.uk/Tools/msa/clustalw2/>). Yellow boxes: minimal PBD-binding motifs. Cl, Dog; Fc, Cat; Bt, Cattle; Hs, Human; Pt, Chimpanzee; Cj, Marmoset; Mm, Mouse; Rn, Rat; Md, Opossum; Oa, Platypus; Gg, Chicken; Xt, Frog; Dr, Fish.

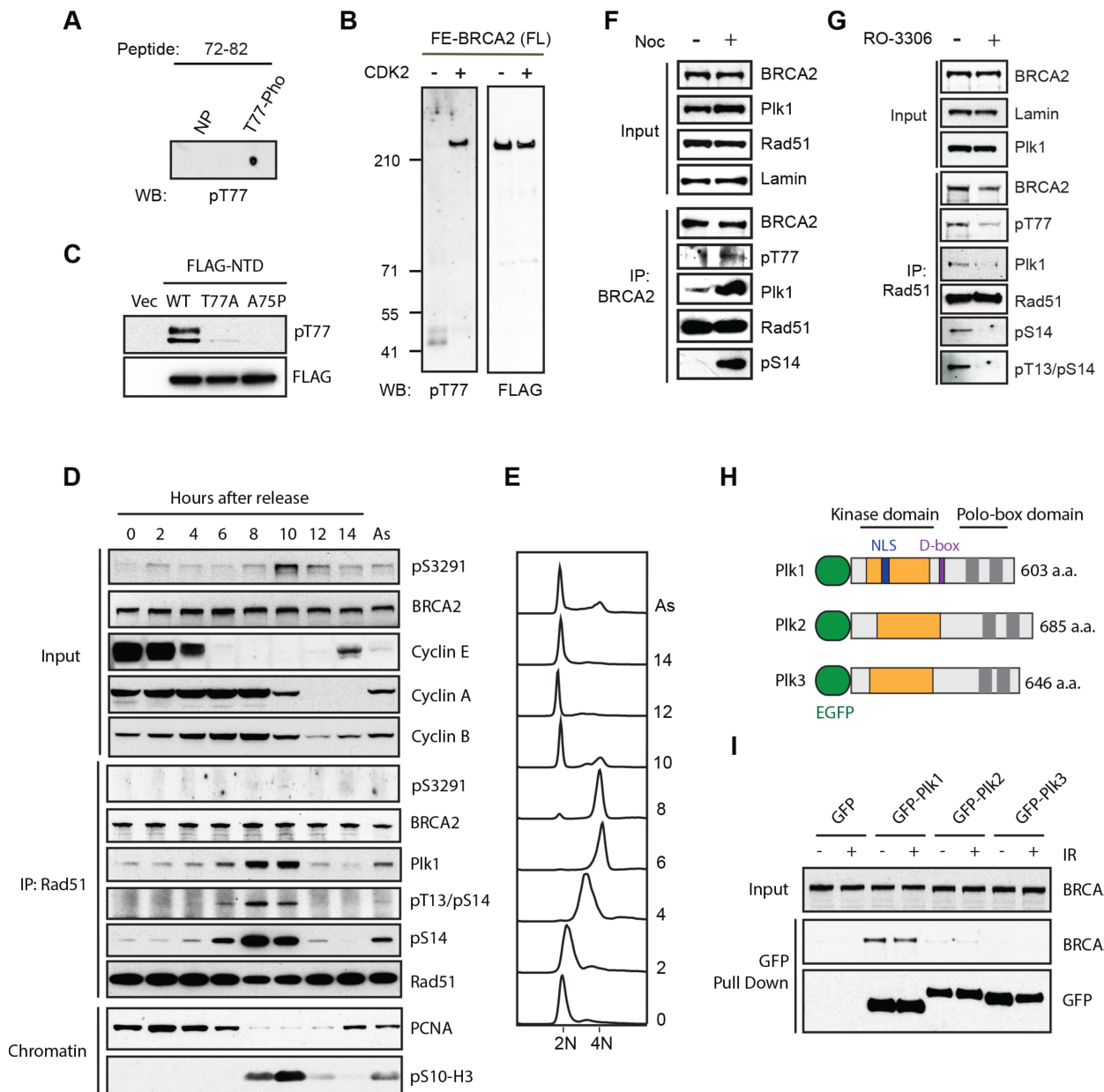


Figure S2, related to Figure 2. Validation and characterization of pT77, and its relationship to Plk1 binding.

(A) Peptide dot blot showing pT77 antibody recognition of phosphorylated (T77-Pho) BRCA2 peptides (amino acid residues 72-82), but not the corresponding non-phosphorylated peptides (NP).

(B) Full length FE-BRCA2 WT (Fig. 1E) affinity purified from HEK293 Flp-In T-REx cells was phosphorylated with recombinant CDK2/cyclin A and blotted using pT77 antibody.

(C) FLAG-NTD variants (Fig. 1D) affinity purified from HEK293T cells was blotted using pT77 antibody.

(D) Detection of S3291 phosphorylation of BRCA2 in synchronized HeLa cells using double thymidine block and release. Rad51 complex in soluble fraction during the cell cycle was also assessed similarly to Fig. 1F.

(E) Flow cytometric analysis of propidium iodide-stained cells.

(F) Western blot analysis of BRCA2 immuno-complex from HeLa cells before and after nocodazole (Noc) treatment.

(G) Western blot analysis of Rad51 immuno-complex from HeLa cells before and after CDK1 inhibitor RO-3306 treatment for 4 hours.

(H) Schematic diagram of Plk1, Plk2 and Plk3 N-terminally tagged with EGFP. Nuclear localization signal (NLS) and destruction-box (D-box) in Plk1 are also indicated.

(I) EGFP-fusions of Plk family member were transiently expressed in HEK293T cells, and following 20 min recovery after irradiation (4 Gy), its association to endogenous BRCA2 was detected following EGFP pull-down.

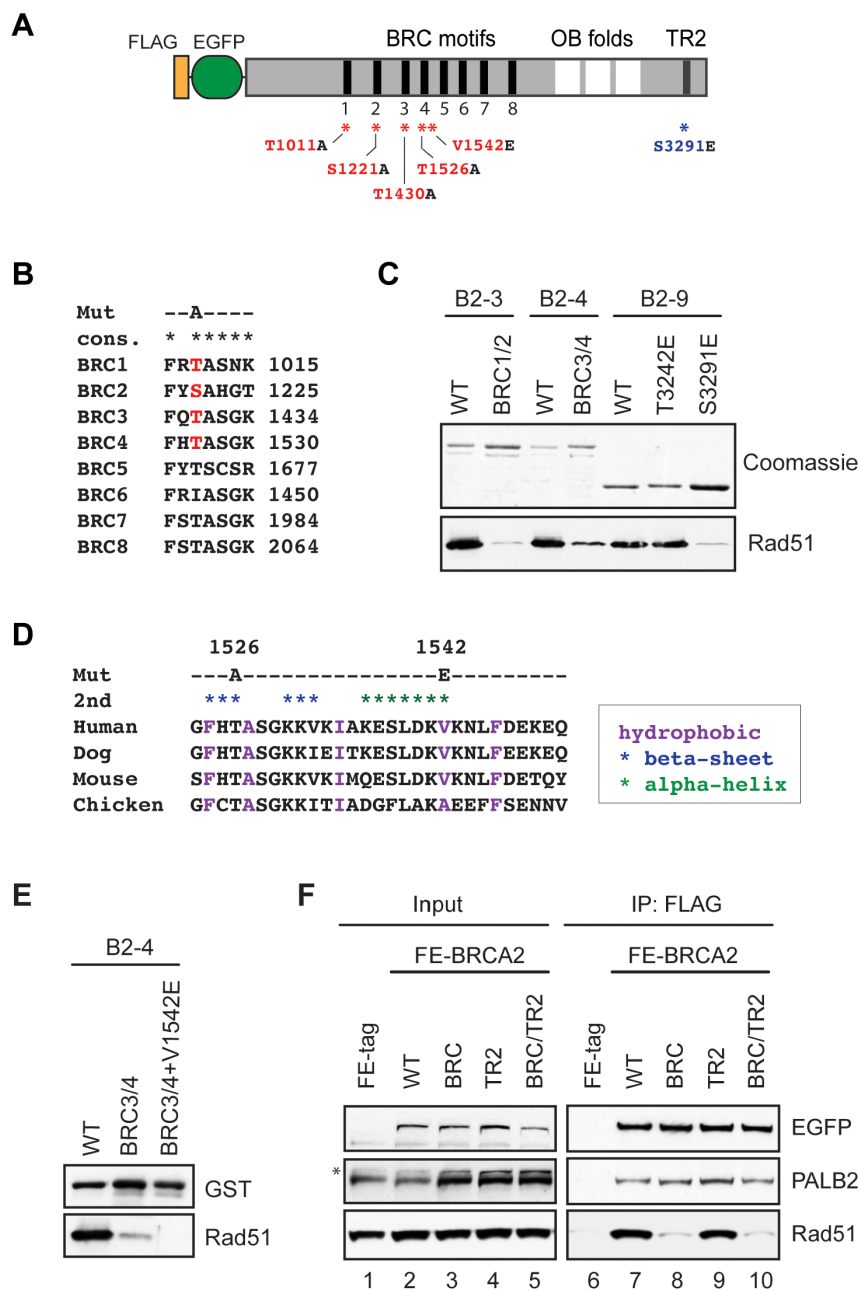


Figure S3, related to Figure 3. Role of BRCA2 in Rad51 phosphorylation at S14.

(A) Schematic diagram of FLAG-EGFP (FE) tagged full-length BRCA2 variants, indicating the FLAG epitope (orange box), EGFP (green rounded box), BRC motifs (black vertical bars), OB folds (white blocks) and TR2 region (grey vertical bar). Introduced amino acid substitutions are indicated by red asterisks (hinder Rad51 binding to BRC motif), and a blue asterisk (hinder Rad51 binding to TR2).

(B-C) Rad51 binding to GST fusions of BRCA2 fragments B2-3, B2-4 and B2-9 shown in Fig. S1A were assessed using recombinant proteins *in vitro* as previously described (Esashi et al., 2005). Note that Rad51 binding to B2-5 was not detectable despite the BRC motifs within the fragment (Esashi et al., 2005; Lee et al., 2004; Thorslund et al., 2007). Highly conserved amino acid residues within BRC1, 2, 3 and 4, highlighted in red, which are proposed to be critical for Rad51 binding (Pellegrini et al., 2002), were substituted to alanine, and its association to Rad51 were

examined following GST pull down. B2-9 with T3291E mutation was used as a negative control for Rad51 binding (Esashi et al., 2005). WT; wild-type, BRC1/2; T1011A/S1221A, BRC3/4; T1526A/F1542A.

(D-E) Additional V1542E mutation within BRC4 was required for complete disruption of B2-4 binding to Rad51 (Lo et al., 2003; Rajendra and Venkitaraman, 2010). Purple residues create a hydrophobic stripe involved in Rad51 binding, and blue and green asterisks indicate residues composing an alpha-helix and a beta-sheet, respectively (Lo et al., 2003).

(F) Full-length BRCA2 constructs with mutations within the BRC and/or TR2 regions were tested for interaction with Rad51. FE-BRCA2 variants were purified by immunoprecipitation with anti-FLAG antibody and interactions with endogenous Rad51 and PALB2 were assessed by western blotting. The asterisk indicates non-specific band detected by the PALB2 antibody.

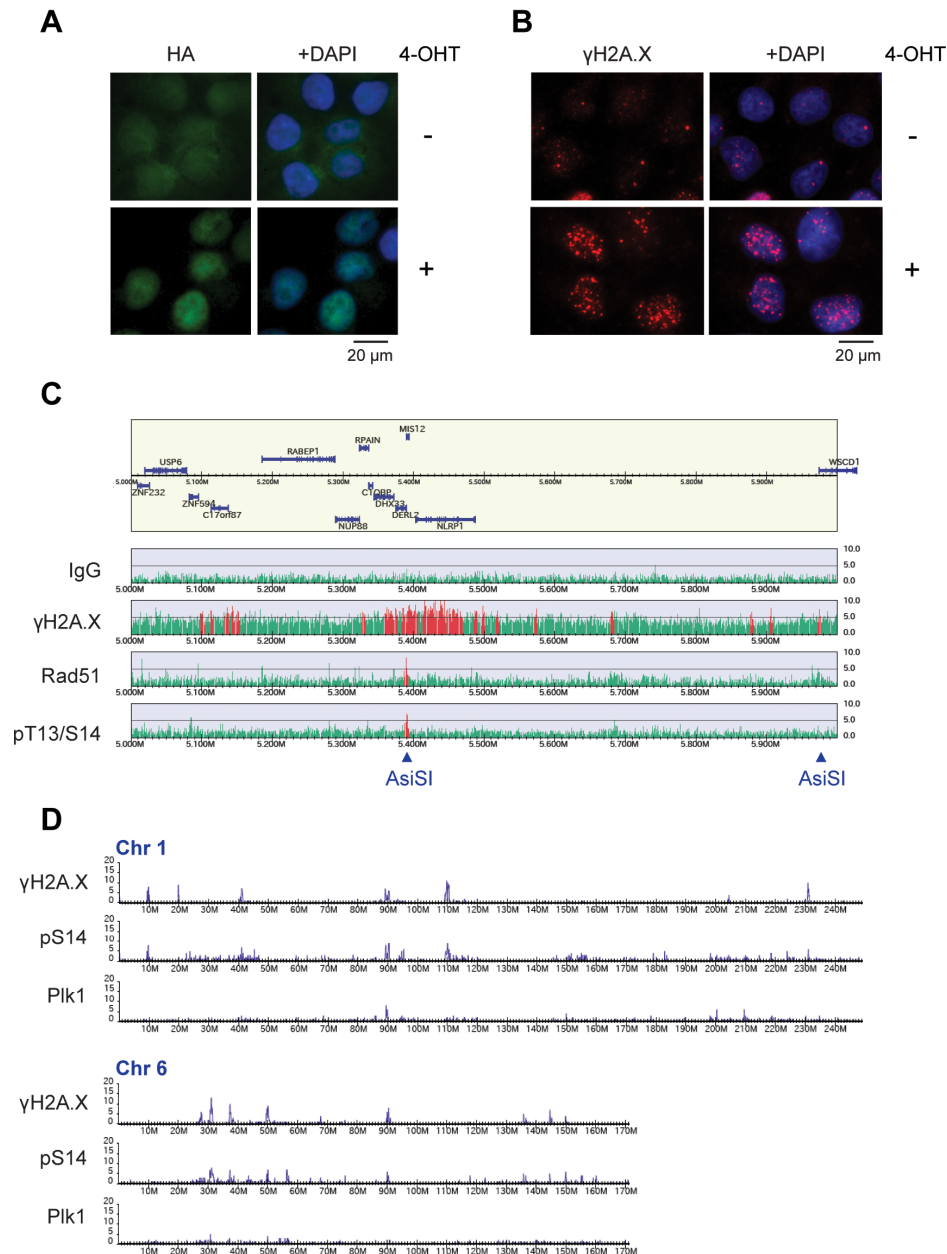


Figure S4, related to Figure 4. ChIP-Seq analyses of phosphorylated Rad51.

(A-B) Representative IF images of U2OS cells stably expressing HA-*AsiSI*-ER fusion before (-) and after (+) 0.3 mM 4-OHT treatment for 4 hours, stained with HA antibody (A) and γ H2A.X antibody (B). Merged images with DAPI staining are also shown on the right panels. The bar indicates 20 μ m.

(C) A ChIP-Seq profile of DNA damage responsive factors at DSB site within chromosome 17, 5-6 Mb, using U2OS *AsiSI*-ER cells treated with 4-OHT for 4 hours, as shown in Fig. 4E. Arrowheads indicate locations containing the *AsiSI* target sequence (GCGATCGC).

(D) Low-resolution views of ChIP-Seq profiles of γ H2A.X, pS14 and Plk1 peaks on chromosome 1 and 6 in U2OS *AsiSI*-ER cells treated with 0.3 mM 4-OHT for 4 hours.

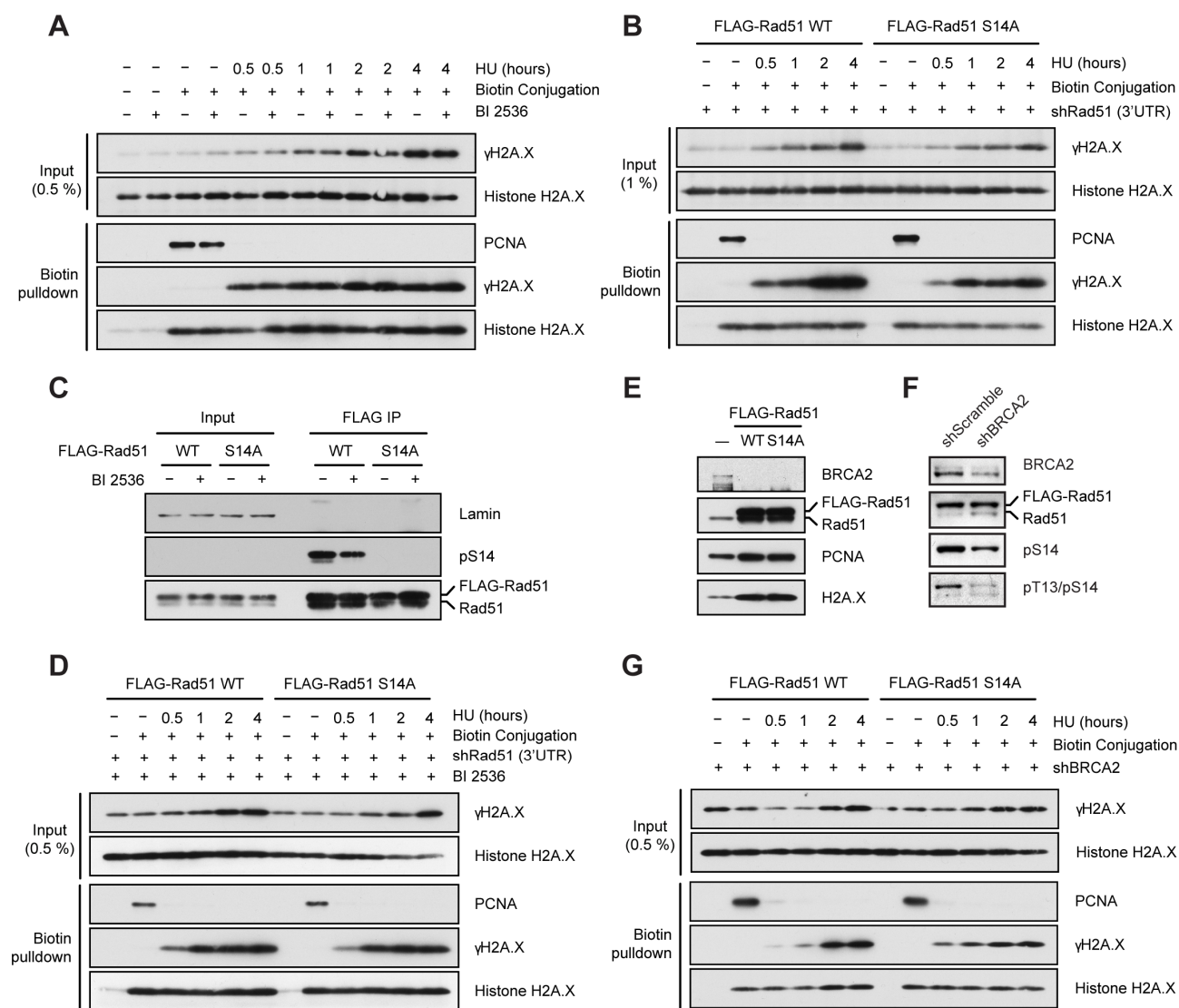


Figure S5, related to Figure 5. Supplementary dataset of iPOND analyses.

(A) Supplementary dataset of iPOND analysis shown in Fig. 5C.

(B) Supplementary dataset of iPOND analysis shown in Fig. 5D.

(C) HEK293 Flp-In T-REx cells conditionally expressing FLAG-tagged Rad51 WT (WT) or Rad51 S14A (S14A) were treated with Plk1 inhibitor BI 2536 for 4 hours, and S14 phosphorylated Rad51 was detected using pS14 antibody.

(D) Supplementary dataset of iPOND analysis shown in Fig. 5E.

(E) HEK293 Flp-In T-REx cells conditionally expressing FLAG-tagged Rad51 WT (WT) or Rad51 S14A (S14A) were treated with shRNA targeting BRCA2, and down-regulation of endogenous BRCA2 was confirmed by western blotting.

(F) Phosphorylation of exogenously expressed Rad51 in HEK293 Flp-In T-REx cells following shRNA mediated down-regulation of endogenous BRCA2 was detected by indicated antibodies.

(G) Supplementary dataset of iPOND analysis shown in Fig. 5F.

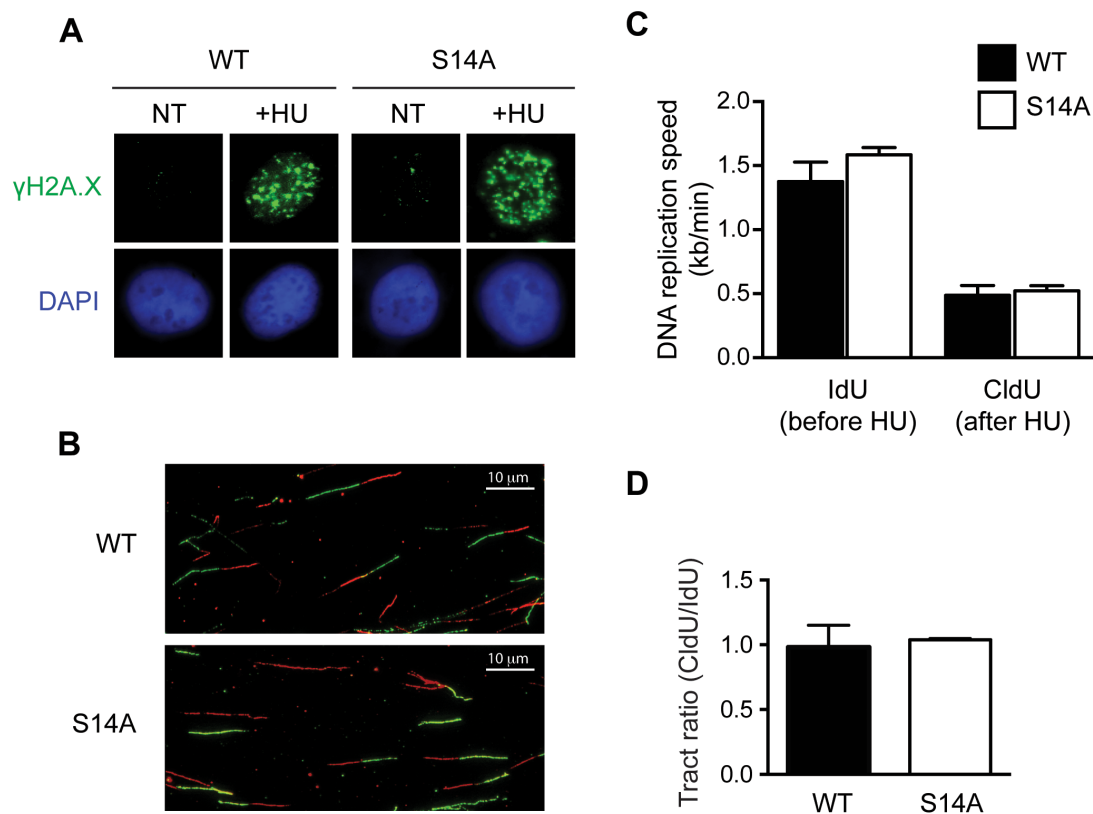


Figure S6, related to Figure 6. Role of Rad51 S14 in response to DNA replication stress.

(A) Representative IF images of HU treated U2OS cells exogenously expressing WT Rad51 or S14A Rad51 after down-regulation of endogenous Rad51. DNA staining with DAPI (blue) and foci detected with γ H2A.X antibody (green) are shown.

(B) Representative wide-field IF images of IdU- and CldU-labeled fibres in HU-treated U2OS cells expressing exogenous WT Rad51 or S14A Rad51 after down-regulation of endogenous Rad51.

(C) IdU- and CldU-labeled fibre lengths were measured from U2OS cells expressing Rad51 WT or Rad51 S14A and treated as described in Fig. 6, and the average DNA synthesis speed was calculated using a conversion factor of $1 \mu\text{m} = 2.59 \text{ kb}$. Error bars, SEM ($n=3$).

(D) IdU- and CldU-labeled fibre lengths were measured from WT and S14A cells treated as above, and relative speeds before and after HU treatment are shown as CldU/IdU ratio. Error bars, SEM ($n=3$).

Table S1. Oligonucleotides and siRNA used for this study

Plk1	Forward 5'-ggggacaagttgtacaaaaagcaggctcctggaagttctgttccaggggccatgagtgctgcagtgactgc-3'
Plk1	Reverse 5'-ggggaccactttgtacaagaagctgggtcctaggaggccttgagacggttgctgg-3'
Plk1-PBD	Forward 5'-ggggacaagttgtacaaaaagcaggctcctggaagttctgttccaggggccatgctcccagcagcctggacc-3'
Plk1-PBD	Reverse 5'-ggggaccactttgtacaagaagctgggtcctaggaggccttgagacggttgctgg-3'
BRCA2 shRNA	Forward 5'-gatcccaacaattacgaaccaaactcaagagagtttggttcgtaattgtgttttc-3'
BRCA2 shRNA	Reverse 5'-tcgagaaaaacaacaattacgaaccaaactccttgaagtttggttcgtaattgtggg-3'
Rad51 shRNA	Forward 5'-gatccccgtgctgcagcctaatagagattcaagagatctcattaggctgcagcactttt-3'
Rad51 shRNA	Reverse 5'-tcgagaaaaagtgtgcagcctaatagagatcttgaatctcattaggctgcagcaggg-3'
EGFP cassette	Forward 5'-ggggacaagttgtacaaaaagcaggcttaggtaccatggtgagcaagggcg-3'
EGFP cassette	Reverse 5'-ggggaccactttgtacaagaagctgggtgctcagggcgccgctggtaccctgtacagctcgt-3'
Primer 1	Forward 5'-cctagtgcagcgtaccagcatataaaaatgactctaggtc-3'
Primer 2	Reverse 5'-ccaagacatatgttgctgatcagtaaatagc-3'
Primer 3	Forward 5'-aagagcggccgatgcctattggtccaaagag-3'
Primer 4	Reverse 5'-ccaagacatatcaggatccacctc-3'
Primer 5	Forward 5'-ggggcatgcaaatagatcccaagtggtccacccaac-3'
Primer 6	Reverse 5'-ggggctcgagttagatataatatttttagttgtaattgtgtcc-3'
T77A	Forward 5'-catctataatcagctggctcagctccaataatattcaaagagcaa-3'
T77A	Reverse 5'-ttgctcttgaatattattggagctgaagccagctgattataagatg-3'
A75P	Forward 5'-ggaaaccatctataatcagctgccttcaactccaataatattcaaa-3'
A75P	Reverse 5'-tttgaatattattggagttgaagcagctgattataagatggttcc-3'
T1011A	Forward 5'-gttttgaggtagcttcagagcagctcaataaggaaatc-3'
T1011A	Reverse 5'-gatttccttattgaagctgctgaagctacctccaaaac-3'
S1221A	Forward 5'-agtggggttagggctttatgctgctcatggca-3'
S1221A	Reverse 5'-tgccatgagcagcataaaagcccctaaacccact-3'
T1430A	Forward 5'-agactctgatacattttcaggctgcaagtgggaaaaatattagt-3'
T1430A	Reverse 5'-actaatattttccactgcagcctgaaaaatgtatcagaagtct-3'
T1526A	Forward 5'-acctactctattgggtttcatgcagctagcggga-3'
T1526A	Reverse 5'-tcccctagctgcatgaaaacccaatagagtaggt-3'
F1542E	Forward 5'-tgcaaaggaatctttggacaaagagaaaaaccttttgatgaaaaag-3'
F1542E	Reverse 5'-cttttcatcaaaaaggttttctttgtccaagattcctttgca-3'
siRad51 3'UTR-1	5'-gacugccaggauaaagcuu-3'
siRad51 3'UTR-2	5'-gugcugcagccuaaugaga-3'

Supplemental References

- Barr, F.A., Sillje, H.H., and Nigg, E.A. (2004). Polo-like kinases and the orchestration of cell division. *Nat Rev Mol Cell Biol* 5, 429-440.
- Bleuyard, J.Y., Buisson, R., Masson, J.Y., and Esashi, F. (2012). ChAM, a novel motif that mediates PALB2 intrinsic chromatin binding and facilitates DNA repair. *EMBO reports* 13, 135-141.
- Burkard, M.E., Randall, C.L., Larochelle, S., Zhang, C., Shokat, K.M., Fisher, R.P., and Jallepalli, P.V. (2007). Chemical genetics reveals the requirement for Polo-like kinase 1 activity in positioning RhoA and triggering cytokinesis in human cells. *Proc Natl Acad Sci U S A* 104, 4383-4388.
- Elia, A.E., Rellos, P., Haire, L.F., Chao, J.W., Ivins, F.J., Hoepker, K., Mohammad, D., Cantley, L.C., Smerdon, S.J., and Yaffe, M.B. (2003). The molecular basis for phosphodependent substrate targeting and regulation of Plks by the Polo-box domain. *Cell* 115, 83-95.
- Esashi, F., Christ, N., Gannon, J., Liu, Y., Hunt, T., Jasin, M., and West, S.C. (2005). CDK-dependent phosphorylation of BRCA2 as a regulatory mechanism for recombinational repair. *Nature* 434, 598-604.
- Jackson, D.A., and Pombo, A. (1998). Replicon clusters are stable units of chromosome structure: evidence that nuclear organization contributes to the efficient activation and propagation of S phase in human cells. *J Cell Biol* 140, 1285-1295.
- Lee, M., Daniels, M.J., and Venkitaraman, A.R. (2004). Phosphorylation of BRCA2 by the Polo-like kinase Plk1 is regulated by DNA damage and mitotic progression. *Oncogene* 23, 865-872.
- Lo, T., Pellegrini, L., Venkitaraman, A.R., and Blundell, T.L. (2003). Sequence fingerprints in BRCA2 and RAD51: implications for DNA repair and cancer. *DNA Repair (Amst)* 2, 1015-1028.
- Pellegrini, L., Yu, D.S., Lo, T., Anand, S., Lee, M., Blundell, T.L., and Venkitaraman, A.R. (2002). Insights into DNA recombination from the structure of a RAD51-BRCA2 complex. *Nature* 420, 287-293.
- Rajendra, E., and Venkitaraman, A.R. (2010). Two modules in the BRC repeats of BRCA2 mediate structural and functional interactions with the RAD51 recombinase. *Nucleic Acids Res* 38, 82-96.
- Schwab, R.A., Blackford, A.N., and Niedzwiedz, W. (2010). ATR activation and replication fork restart are defective in FANCM-deficient cells. *EMBO J* 29, 806-818.
- Thorslund, T., Esashi, F., and West, S.C. (2007). Interactions between human BRCA2 protein and the meiosis-specific recombinase DMC1. *EMBO J* 26, 2915-2922.
- Yata, K., Lloyd, J., Maslen, S., Bleuyard, J.Y., Skehel, M., Smerdon, S.J., and Esashi, F. (2012). Plk1 and CK2 act in concert to regulate Rad51 during DNA double strand break repair. *Molecular cell* 45, 371-383.